# Proposal for a $1\times3$ Goos-Hänchen shift-assisted de/multiplexer based on a multilayer structure containing quantum dots

H. Sattari, S. Ebadollahi-Bakhtevar, and M. Sahrai

Citation: Journal of Applied Physics **120**, 133102 (2016); doi: 10.1063/1.4964443
View online: https://doi.org/10.1063/1.4964443
View Table of Contents: http://aip.scitation.org/toc/jap/120/13
Published by the American Institute of Physics

# Proposal for a 1×3 Goos-Hänchen shift-assisted de/multiplexer based on a multilayer structure containing quantum dots

H. Sattari,[1,a)] S. Ebadollahi-Bakhtevar,[2] and M. Sahrai[3]
[1]*Nanotechnology Research Center, Bilkent University, Ankara 06800, Turkey*
[2]*Young Researchers and Elite Club, Tabriz Branch, Islamic Azad University, Tabriz 51589, Iran*
[3]*Research Institute for Applied Physics and Astronomy, University of Tabriz, Tabriz 51665-163, Iran*

(Received 9 July 2016; accepted 25 September 2016; published online 6 October 2016)

A multilayer structure with the wavelength selective features based on Goos-Hänchen (GH) shift is proposed and investigated. We present a layered media containing quantum dots for active control of the GH shift for the reflected light. This configuration includes a distributed Bragg reflector to have minimum optical power transmission to the substrate. In addition, a passive cladding layer is used to enhance the total lateral shift for the reflected beams. For a fixed structure and incident angle, our results demonstrate that by proper manipulation of the optical properties and susceptibility of the active layer, de/multiplexing capabilities of such a device could be controlled. This type of grating-less device can be used as a compact wavelength division multiplexing system with actively controllable channel spacing. We demonstrate possibility of a 1 × 3 de/multiplexer with channel spacing of 2 nm. *Published by AIP Publishing*. [http://dx.doi.org/10.1063/1.4964443]

## I. INTRODUCTION

One of the most promising concepts for high capacity communication systems is wavelength division multiplexing (WDM). WDM technique makes a low-cost method for extending information transmission capacity and increasing network design flexibility.[1,2] Of the important components in WDM transmission system are de/multiplexers. In past two decades, most of the theoretical studies in WDM systems involving de/multiplexers which are devoted to prisms, thin film filters, and diffraction gratings have rapidly increased.[3–5] Recent developments in characterization and fabrication of nano-scale devices have triggered efforts to realize emerging compact telecommunication devices such as quantum wells and dots. Nano-scaled semiconductor quantum dots (QDs) are collections of thousands of atoms with confined charge carriers in three dimensions. QDs have found special attention because of their similar properties to atomic vapours, but with the advantage of flexible design and controllable energy diagram. A device which takes the advantage of the inter-subband transitions in QDs has inherent advantages such as high nonlinear optical coefficients, large electric dipole moments (due to the small effective electron mass), and a great flexibility in device design by a proper selection of the materials and their sizes. In recent years, quantum optical phenomena based on quantum coherence have attracted a lot of attention in QDs.[6–8] Moreover, because of the three-dimensional confinement of carriers in QDs, they exhibit quantum optical behaviour for incident light with any direction.

The confinement of carriers, large nonlinear response, and easily controllable size and energy levels spacing make QD molecules appropriate candidates for optical integrated studies such as ultra-narrowband switches and filters.

An interesting wave optics effect is the Goos-Hänchen (GH) shift. When a beam of electromagnetic wave is obliquely incident on boundary of two media with different refractive indices, the reflected and transmitted light beams experience a lateral shift from the ideal position predicted by beam optics. This phenomenon is known as the Goos-Hanchen shift. The optical processes related to the GH shift have shown potential in possible optoelectronic applications, such as optical heterodyne sensors for measuring refractive index, temperature and film thickness sensor devices,[9] and optical switching.[10] The GH shift has been investigated in several optical structures such as cavities containing atomic medium,[11,12] photonic crystals (PCs),[13,14] semiconductors,[15] metals[16–18] and negative refractive index media.[19] Some efforts have been made for enlarging magnitude of the GH shift. For example, Lai and Chan used absorbing semi-infinite media for TM-polarized waves and obtained a large and negative Goos-Hänchen shift near the Brewster angle.[20] Yang *et al*. have studied possibility of giant GH shift in a cavity comprising coupled quantum wells. They have controlled this shift through the tunnelling-induced quantum interference effect.[21]

In the current work, we use the GH shift to design a three channel de/multiplexer by the assist of a sub-layer doped with QDs. By proper selection of the rate of incoherent optical field, the proposed model can be effectively able to multiplex and demultiplex reflected pulse with channel spacing of 2 nm.

## II. MODEL AND EQUATIONS

Consider a multilayer medium as the body of de/multiplexing device (Fig. 1). The structure includes four parts: titanium oxide cladding layer with thickness of 20.3 $\mu$m and refractive index of 2.22, active layer containing QDs with thickness of 3.75 $\mu$m, distributed Bragg reflector (DBR), and a InP(311)B substrate with refractive index of 3.15. DBR

[a)]Electronic mail: sattari@tabrizu.ac.ir

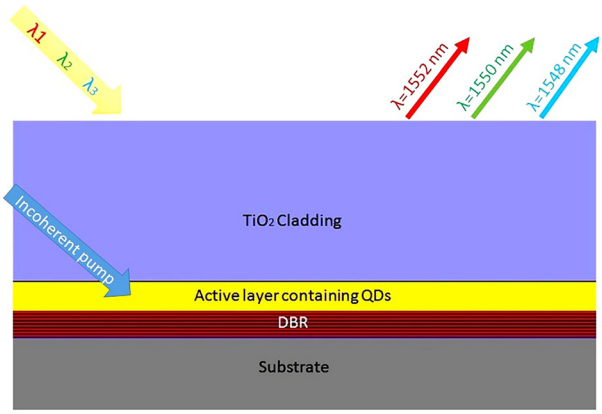


FIG. 1. Sketch of the proposed multilayer medium for optically controllable de/multiplexing.

layer lays under the active layer and it consists of seven couple of silica/silicon layers with refractive indices of 1.44 and 3.42, respectively. The thicknesses of each silica and silicon layer are set to be 0.28 $\mu$m and 0.12 $\mu$m, respectively. With such a choice, we guarantee a wide angle high reflection for wavelengths around $\lambda_0 = 1550\,\text{nm}$ from proposed layered media.

Suppose that the active layer is a stack of InAs QDs embedded in InGaAlAs grown on an InP(311)B substrate by molecular beam epitaxy. Through the growing process, one may engineer the structure to have a QD resembling a three-level ladder type atom having a transition in telecommunication window.[22] A possible layout for such an active layer is depicted in Fig. 2(a). In addition, Fig. 2(b) shows a ladder composition for energy levels of the QDs.

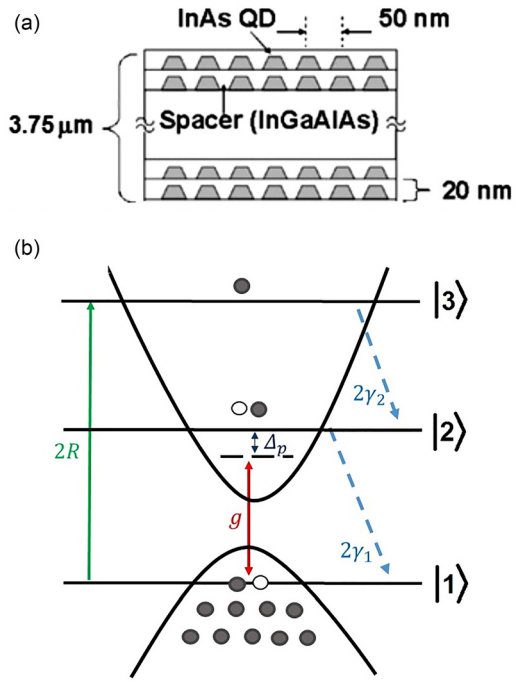


FIG. 2. (a) Structure and average QD size of the sample for the active layer. (b) Energy diagram for a QD in which a ladder composition could be determined.

A weak probe laser field with the frequency $\omega_p$ and the Rabi-frequency of $g = \frac{\vec{\mu}_{12}.\vec{E}_p}{\hbar}$ is applied to the transition $|1\rangle \leftrightarrow |2\rangle$, while the transition $|1\rangle \leftrightarrow |3\rangle$ is pumped by an incoherent pumping field with the amplitude $\varepsilon$ and the pumping rate of $2R = 2(\mu_{13}^2/\hbar^2)\Gamma_P$.[23] Here, $\mu_{ij}$ and $E_p$ are the corresponding electric dipole moments and the amplitude of the applied laser field. $2\gamma_1$ and $2\gamma_2$ denote the spontaneous decay rates from level $|2\rangle$ to $|1\rangle$ and level $|3\rangle$ to $|2\rangle$, respectively. Note that the total decay rates $\gamma_1$ and $\gamma_2$ are comprised of a population decay contribution as well as a dephasing contribution. The equations of motion in rotating frame and rotating wave approximation for the system can be written as follows:

$$\begin{aligned}
\dot{\tilde{\rho}}_{11} &= -2R\rho_{11} + 2\gamma_1\rho_{22} + ig^*\rho_{21} - ig\rho_{12},\\
\dot{\tilde{\rho}}_{22} &= 2\gamma_2\rho_{33} - 2\gamma_1\rho_{22} - ig^*\rho_{21} + ig\rho_{12},\\
\dot{\tilde{\rho}}_{33} &= 2R\rho_{11} - 2\gamma_2\rho_{33},\\
\dot{\tilde{\rho}}_{12} &= -(R + \gamma_1 + i\Delta_p)\rho_{12} + ig^*(\rho_{22} - \rho_{11}),\\
\dot{\tilde{\rho}}_{13} &= -[R + \gamma_2 + i(\Delta_p + \omega_{23})]\rho_{13} + ig^*\rho_{23},\\
\dot{\tilde{\rho}}_{23} &= -(\gamma_1 + \gamma_2 + i\omega_{23})\rho_{23} + ig\rho_{13},
\end{aligned} \tag{1}$$

where $\tilde{\rho}_{11} + \tilde{\rho}_{22} + \tilde{\rho}_{33} = 1$ and $\rho_{ij} = \rho_{ji}^*$. Here, the detuning parameter for the probe field is defined as $\Delta_p = \omega_{21} - \omega_p$. The parameter $\omega_{ij}$ is the frequency difference between level $|i\rangle$ and level $|j\rangle$. Solving the equations of motion at the steady state leads to dispersion and absorption spectra, which are determined by the real and imaginary parts of susceptibility as

$$\chi = \frac{2N\mu_{12}}{\varepsilon_0 E_P}\tilde{\rho}_{21}. \tag{2}$$

Here, $\tilde{\rho}_{21}$ and $N$ are the coherence terms of density matrix for levels $|1\rangle$ and $|2\rangle$ in the rotating frame, and the density of carriers in the QDs sample, respectively.

For the proposed system, we consider the TE-polarized probe beam $E_p$ at an incident angle $\theta$ with central wavelength of $\lambda_0 = 1550\,\text{nm}$, and we calculate the reflection for a light pulse using the transfer matrix method.[24] We also use a finite element solver COMSOL Multiphysics for numerical simulation of the lateral shifts. According to the stationary-phase approach, longitudinal lateral shift known as the Goos-Hänchen shift for the reflected beams is calculated as[25,26]

$$S_r = -\frac{\lambda}{2\pi}\frac{d\varphi_r}{d\theta}, \tag{3}$$

where $\lambda$ is the wavelength, and $\varphi_r$ is the phase of reflection coefficient. We can express the lateral shift of the reflected beam through the relation

$$S_r = -\frac{\lambda}{2\pi|r(\omega)|^2}\left\{\text{Re}[r(\omega)]\frac{d\text{Im}[r(\omega)]}{d\theta} - \text{Im}[r(\omega)]\frac{d\text{Re}[r(\omega)]}{d\theta}\right\}, \tag{4}$$

where $r$ is the complex reflection coefficient that could be calculated through the transfer matrix method.

## III. RESULT AND DISCUSSION

Based on Eq. (1), we analyze numerically the behavior of lateral shifts for three incident optical fields with wavelengths of 1548 nm, 1550 nm, and 1552 nm. For QDs inside the active layer, we assume the decay rate of transitions, the electric dipole moment, and the density of carriers to be $\gamma_1 = \gamma_2 = \gamma = 10^{11}(\mathrm{Hz})$, $\mu_{21} = 0.2 \times 10^{-27}(\mathrm{C\,m})$, and $N = 0.75 \times 10^{21}(\mathrm{m}^{-3})$, respectively. We consider that the central wavelength of the probe beam $\lambda_0$ coincides with the related wavelength for the transition $|1\rangle \leftrightarrow |2\rangle$. In such a condition ($\Delta_p = 0$), the central wavelength will be in resonance with the quantum system illustrated in Fig. 2(b). We investigate the GH shift behavior in incidence angles from 35° to 40°. For smaller angles, the reflected intensities for different wavelengths would not attain proper separation for coupling to separate channels, and it would lead to a considerable crosstalk. On the other hand, for bigger angles, the shifted reflected pulse would become substantially wide, and next to pulse distortion, we would have high crosstalk.

First, we plot the lateral shifts for the reflected light with respect to the incidence angle when there is no incoherent pumping, i.e., $R = 0$. As specified with a gray box in Fig. 3(a), there is a region around $\theta = 39°$ that the shift profiles for the entire incident wavelengths behave nearly linear with a constant amplitude difference with respect to each other. This shift difference is equal to $\Delta\lambda = 2\lambda_0 = 2 \times 1550(\mathrm{nm})$. For $\theta = 39°$, the lateral shifts for wavelengths 1548nm, 1550 nm, and 1552 nm are $18\lambda_0$, $16\lambda_0$, and $14\lambda_0$, respectively. This difference in lateral shifts for different wavelengths is originated from dispersion characteristics of the active layer as there is a resonance condition for $\lambda = \lambda_0 = 1550$ nm and an off-resonance condition for two other waves. In order to show the de/multiplexing characteristics of the device, we seek for an approach to have equal lateral shifts for every wavelength. To do this, we consider the effect of incoherent pumping field. By applying an incoherent optical pumping to the active layer, we can manipulate the susceptibility of the QDs. This way, the complex reflection coefficient of the system can be engineered. Consequently, the lateral shift for reflected pulse could be manipulated.

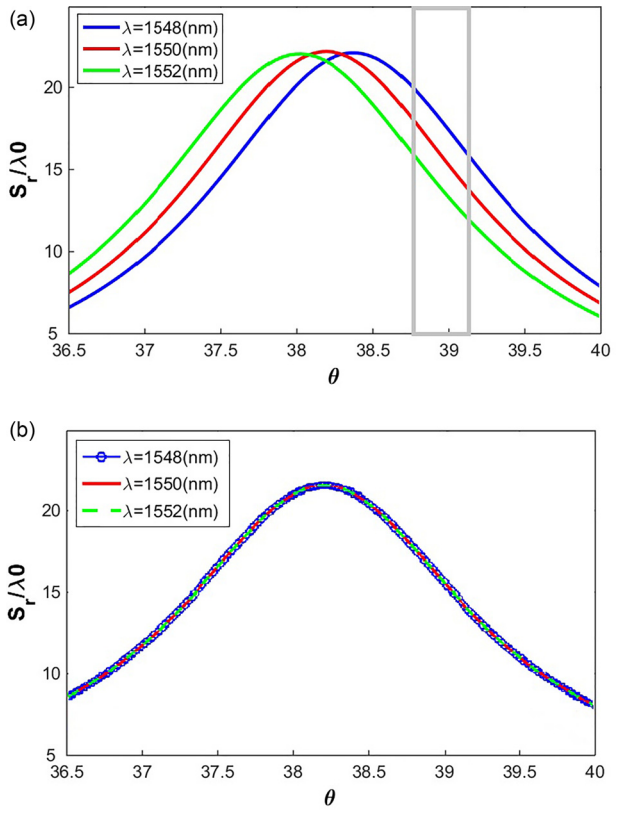


FIG. 3. Normalized lateral shift for reflected beam for three distinct wavelengths versus incidence angle when the rate of incoherent pumping is (a) $R = 0$ and (b) $R = 2\gamma$.

An interesting result is that as the incoherent pumping rate increases, the reflected lateral shift curves for each three channels in all incident angles become close together. When we apply an incoherent optical pumping with the rate of $R = 2\gamma$ to the active layer, we could match the GH shift curves of three incident wavelengths together as shown in Fig. 3(b). Physically, increasing the incoherent pumping field causes to more transfer of population from the ground level to the level $|3\rangle$. Then, this population decays to the level $|2\rangle$. Under this condition in collection of QDs within the active layer, the population of QDs with the occupied ground level will considerably decrease. Therefore, the probability of absorption from the ground level to the level $|2\rangle$ for the probe field will substantially diminish. This happens whether or not the probe field is with resonance wavelength or off-resonance wavelength. In fact, for $R = 2\gamma$, the layered medium exposes similar dispersion characteristic for three incident wavelengths. In other words, the incident beams for three wavelengths have similar behaviors in output, and in this case, the curves are coincident. Therefore, by having an input channel directed about $\theta = 39°$ with respect to the normal to the layered medium, we can optically control the de/multiplexing process for three wavelengths: 1548 nm, 1550 nm, and 1552 nm.

Next, we present simulations performed by finite element solver for verifying the former results. We consider a beam with spatial Gaussian profile incident from air to the layered medium. Fig. 4 shows the simulation result for a beam with a width of $w = 4\lambda_0$ and an incident angle of $\theta = 39°$. Small physical spacing between the output channels is desired for the proposed device. Beams with larger waist bear less deformation after the reflection. However, in such a case, we will need large output channels which could cause to a large device with probable multimode effects in waveguiding. Here, we first have verified the slowly varying behavior of the reflection coefficient and then have selected the waist of the input beam as $4\lambda_0$. This is an optimum choice according to physical constrains and issues related to the application. The beams with large waist need wider waveguide apertures, although they suffer less from deformation. The beams with smaller waist are prone to deformation, but they could have more efficient coupling to the output channels. As it is apparent from the figures, the passive titanium oxide cladding layer assists to have enlarged lateral shift from the surface of the device. This way we elude the interrupting interference effects in output channels. Fringes in the pattern of electrical field intensity are due to

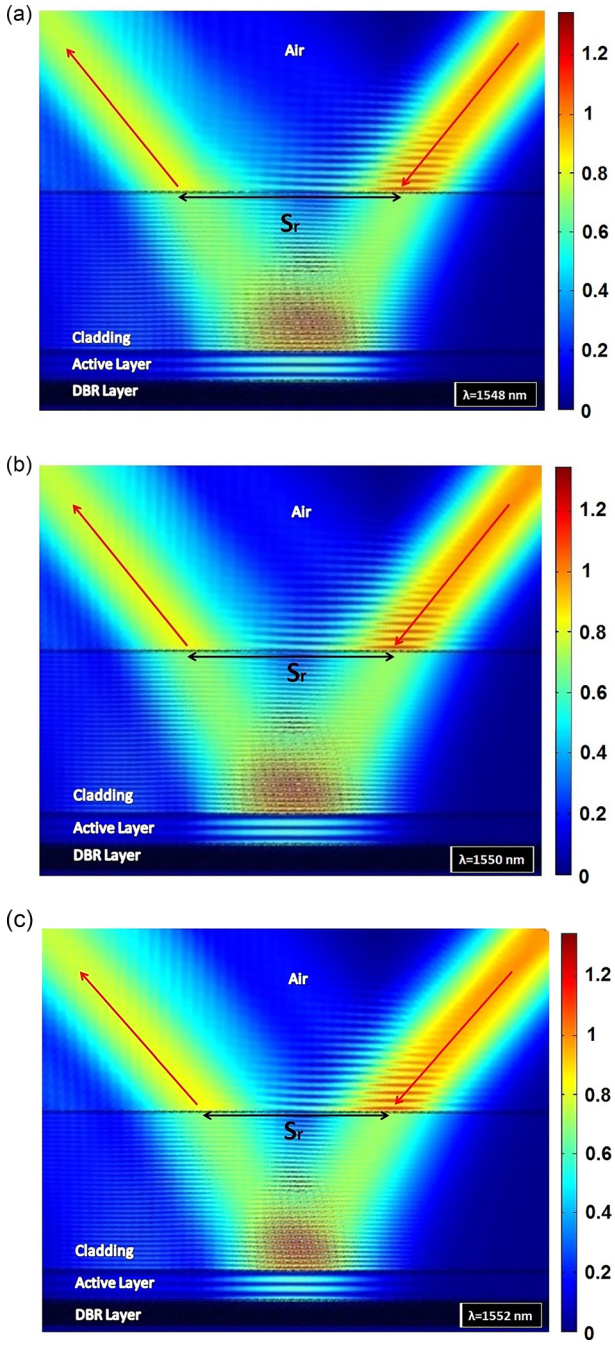


FIG. 4. Numerical study results for normalized electrical field intensity pattern when the Gaussian beam is incident from air. (a) $\lambda = 1548\,\text{nm}$ and $S_r = 18\lambda_0$,(b) $\lambda = 1550\,\text{nm}$ and $S_r = 16\lambda_0$, and (c) $\lambda = 1552\,\text{nm}$ and $S_r = 14\lambda_0$. The incidence angle is $\theta = 39°$, the Gaussian beam width is $w = 4\lambda_0$, and $R = 0$ for all the cases.

interference between the incident and reflected waves from boundaries of the layers.

To estimate required space for designing physical output channels and waveguides, we plot the distribution of electrical field intensity cross-section on a plane perpendicular to wave vector of the reflected beam. Fig. 5 shows a maximum of about 0.37 for reflected normalized intensities. It can be estimated that having three waveguides with width of 2 $\mu$m separated by 1 $\mu$m from each other, the coupling efficiency would be acceptable. There are also two small side peaks in the profile of the intensities. The right peak is due to reflection from

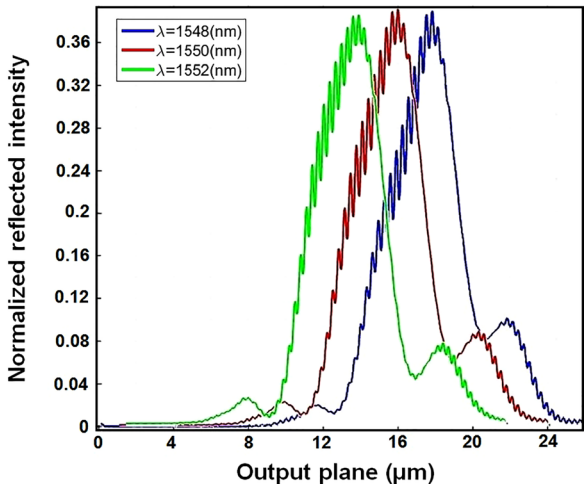


FIG. 5. Profiles of the reflected beams for three discussed wavelengths on the output channel plane.

the interface of air and cladding layer, and the left peak in the profile is because of the interference effect near the surface of the medium. Note that this design includes a passive cladding layer. This layer keeps the output channels away from the active interference region. As it is apparent from Fig. 4, in the vicinity of every reflecting interface, we discern interference fringes which could modulate the reflected beam and cause to beam deformation. However, this layer itself reflects some portion of the input power before its interaction with the active region. This has two consequences: first, reduction of the output signal amplitude, and second, introducing an excessive slope peak to the profile of the reflected beam. One may engineer the layers to diminish or even amplify these peaks according to the expected application. The average out-of-band crosstalk for channels is calculated to have a value of 2.5 dB, which is acceptable for the proposed $1 \times 3$ de/multiplexing system. To increase the capacity of the channel, we need to have more output channels with narrower channel spacing. However, the channel spacing of the proposed device is acceptably narrow, and the number of output channels is still low. To overcome this, one may use an array, including multiple of this device. In that case, the optimum parameters for the optical and geometrical parameters should be selected to minimize the crosstalk and insertion loss of the system.

## IV. CONCLUSION

In conclusion, a grating-less $1 \times 3$ multilayer de/multiplexer with a channel spacing of 2 nm and a central wavelength of $\lambda_0 = 1550\,\text{nm}$ is proposed, and its functionality is investigated both numerically and with simulation. The active layer of the device contains QDs which their susceptibility could be manipulated optically through an incoherent optical pumping. By having active optical control over the GH shift of the reflected beam and with the assist of a cladding layer, we could define three distinct separate channels. The characteristics such as accessible controllable geometrical and optical parameters make the proposed model a potential candidate for active real-time integrated optics applications.

[1]B. Mukherjee, IEEE JSAC **18**, 1810 (2000).
[2]R. Ramaswami, K. Sivarajan, and G. Sasaki, *Optical Networks: A Practical Perspective* (Morgan Kaufmann, 2009).
[3]A. Grosso, E. Leonardi, M. Mellia, and A. Nucci, IEEE Commun. Lett. **5**, 172 (2001).
[4]M. K. Smit and C. Van Dam, IEEE J. Sel. Top. Quantum Electron. **2**, 236 (1996).
[5]B. Pezeshki, F. K. Tong, J. A. Kash, D. W. Kisker, and R. M. Potemski, IEEE Photonics Technol. Lett. **5**, 1082 (1993).
[6]J. R. Petta, A. C. Johnson, J. M. Taylor, E. A. Laird, A. Yacoby, M. D. Lukin, C. M. Marcus, M. P. Hanson, and A. C. Gossard, Science **309**, 2180 (2005).
[7]D. Birkedal, K. Leosson, and J. M. Hvam, Phys. Rev. Lett. **87**, 227401 (2001).
[8]J. M. Villas-Bôas, A. O. Govorov, and S. E. Ulloa, Phys. Rev. B **69**, 125342 (2004).
[9]T. Hashimoto and T. Yoshino, Opt. Lett. **14**, 913 (1989).
[10]T. Sakata, H. Togo, and F. Shimokawa, Appl. Phys. Lett. **76**, 2841 (2000).
[11]S. Qamar and M. S. Zubairy, Phys. Rev. A **81**, 023821 (2010).
[12]S. Asiri, J. Xu, M. Al-Amri, and M. Suhail Zubairy, Phys. Rev. A **93**, 013821 (2016).
[13]D. Felbacq and R. Smaâli, Phys. Rev. Lett. **92**, 193902 (2004).
[14]P. Hou, Y. Chen, X. Chen, J. Shi, and Q. Wang, Phys. Rev. A **75**, 045802 (2007).
[15]C. Luo, J. Guo, Q. Wang, Y. Xiang, and S. Wen, Opt. Express **21**, 10430 (2013).
[16]X. Yin and L. Hesselink, Appl. Phys. Lett. **89**, 261108 (2006).
[17]P. T. Leung, C. W. Chen, and H.-P. Chiang, Opt. Commun. **276**, 206 (2007).
[18]M. Merano, A. Aiello, M. P. Van Exter, E. R. Eliel, and J. P. Woerdman, Opt. Express **15**, 15928 (2007).
[19]P. R. Berman, Phys. Rev. E **66**, 067603 (2002).
[20]H. M. Lai and S. W. Chan, Opt. Lett. **27**, 680 (2002).
[21]W. X. Yang, S. Liu, Z. Zhu, and R. K. Lee, Opt. Lett. **40**, 3133 (2015).
[22]J. Inoue, T. Isu, K. Akahane, and M. Tsuchiya, Appl. Phys. Lett. **89**, 151117 (2006).
[23]K. T. Kapale, M. O. Scully, S. Y. Zhu, and M. S. Zubairy, Phys. Rev. A **67**, 023804 (2003).
[24]C. C. Katsidis and D. I. Siapkas, Appl. Opt. **41**, 3978 (2002).
[25]M. McGuirk and C. K. Carniglia, J. Opt. Soc. Am. **67**, 103 (1977).
[26]L. G. Wang, H. Chen, and S. Y. Zhu, Opt. Lett. **30**, 2936 (2005).